Simulation of a free falling wedge into water using 2D CFD with applications in the prediction of high speed craft motions

Lewis, S.G., Hudson, D.A., Turnock, S.R.

Fluid Structure Interactions Research Group, School of Engineering Sciences,

University of Southampton, Southampton, SO17 1BJ, UK

Email: sgl101@soton.ac.uk

1. Introduction

Small boats are often required to operate at as high a speed as possible. The crew experience repeated shocks and vibration, which can lead to a reduction in their physical and mental performance. Accurate prediction of the motions of high speed craft is an essential element in understanding the response of the crew to a particular design configuration. The problem of predicting planing craft performance and motions is currently solved using one of two principal methods:

The first numerical method uses a two dimensional (2D) potential flow theory to calculate the forces associated with wedge entry in order to evaluate the added mass and damping terms in the equations of motion. Previous work has been conducted using a non-linear potential flow model (Lewis et al, 2006).

The second numerical method, uses computational fluid dynamics (CFD) to solve the full three dimensional (3D) Reynolds averaged Navier Stokes equations (RANSE). This 3D CFD method has been applied to solve the motions of sailing yachts (Azcueta, 2002), planing craft (Azcueta, 2003) and ships in waves (Sato, 1999), with good results. The computational cost of such simulations is significant, despite continual increases in computational power. When predicting the motions of a planing craft in waves, Azcueta (2003) states that a 2s simulation had a processing time of 33 hours on a single processor computer.

Another possible method to predict high speed craft motions is to introduce a hybrid model making use of both a RANSE method and the 2D strip theory discussed by Lewis et al (2006). A simulation that predicts wedge impacts accurately with 2D CFD can be developed and a series of wedges applied to create a 3D hull. Overall craft motions may then be calculated in a similar manner to the 2D potential solver.

2. CFD Techniques

There are a number of methods that can be applied to simulate a wedge impacting with water. One method incorporates a moving mesh, where the mesh is attached to the surface of a ship and deforms as the ship moves. The grid system is also fixed to the free surface. This approach is adopted by Akimoto (2002) and Ohmori (1998). Sato et al (1999) note that this method cannot cope readily with large amplitude motions. Another method used to predict ship motions using CFD is to use a fixed co-ordinate system introducing the body forces on the ship into the external force component of the Navier-Stokes equations. This method is adopted by Sato et al (1999).

This investigation uses a commercial RANSE solver (Ansys CFX, 2007) to calculate wedge impacts with water. A body-fixed mesh is used, and the movement of the body is realized by altering the level of the free surface. For the case of a 2D wedge impact, only one degree of freedom is investigated: the vertical motion. The lower boundary of the computational domain is defined as an opening and the water inflow velocity is set as the instantaneous wedge vertical velocity. This method of simulating wedge impact has the advantage of requiring only one mesh, which can be refined in areas of interest, such as the apex of the wedge and the wall water jets expected as the water level rises. A high density of mesh cells is required in the vertical direction so that the mean free surface location is well captured. The timestep is chosen ensuring that the maximum Courant number is approximately 1. The Courant number is a non-dimensional

variable that is defined as the ratio of the distance the flow moves in each time step to the number of mesh elements that are crossed over this distance. The flow at critical locations, such as the wedge apex, will therefore have a Courant number of much less than 1.

2.1 Turbulence Models

For the required typical small boat slams the flow along the wedge will be viscous. The typical Reynolds number for wedge entry, calculated from data presented by Yettou et al (2006) is $6x10^6$. A suitable turbulence model is required to close the Navier-Stokes equations. Three approaches are investigated to examine the dependence on the method of closure. Initially, the default *k-ε* turbulence model is used, as it is well known and understood. The two equations governing this turbulence model can be found in Launder and Spalding (1974).

The k-ε model is sensitive to the near-wall grid resolution which is assessed in the dimensionless wall unit y+, which for an unsteady flow is time varying. The near-wall resolution should be such that y+ is always greater than 30 (WS Atkins, 2003). An improvement to the *k-ε* model is the Renormalization-Group-Based (RNG) k- ε model. This has an additional term that significantly improves the accuracy for rapidly strained flows, making it more accurate for a larger range of flows than the standard k- ε model.

The shear stress transport (SST) *k-ω* model was developed by Menter (1994). This model provides an enhanced near wall simulation but requires the first mesh cell to have a $y^+ \approx 1$. All the models require the specification of *k* and either ε or *ω* on the inlet boundaries, for which the default solver values were used.

2.2 Computational Time

The computational time is dependant on the number of mesh elements, the number of time steps and the desired solution accuracy. The computer used to solve the simulation has a Pentium 4, 3.2 GHz processor, with 2Gb of random access memory. With a coarse grid containing around 9000 elements, to solve a flow in about 500 time steps takes a wall clock time of approximately 2.5 hours. For these calculations convergence at each time step was deemed to have occurred when the mass residual for this particular simulation was less than an RMS value of $5x10^{-6}$.

3. Free Falling Wedge Entry

The initial investigation assumed that the impact velocity of the wedge was constant, that is to say, on actual impact the induced force did not reduce the imposed velocity. The simulation was then altered to allow the velocity of the wedge to change during impact. The computational domain is set as a multi-phase problem containing ideal air and water. Ideal air is considered to be a compressible homogeneous fluid by the solver. It has isothermal properties, meaning that the pressure is directly proportional to the density. The amount of each substance in each cell is defined by a volume fraction for that cell. The inflow at the bottom of the computational domain is defined as having a water volume fraction of 1, and an air volume fraction of 0. The RANSE solver locates the level of the free surface by determining the position within a cell that has a volume fraction of 0.5 for each substance.

3.1 Simulation

Initially, a 2D wedge impact is simulated in calm water. The commercial RANSE solver does not support true 2D flow, although a 3D mesh can be constructed that is one cell thick. In effect this is a 2D mesh as there is no flow in the direction of the third dimension. A structured coarse mesh is constructed to enable the overall simulation to be initialised and results obtained relatively quickly. The coarse mesh for a wedge with a deadrise angle of 25° is presented in figure 1.

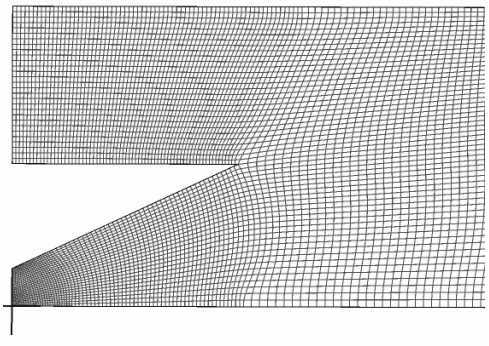

Figure 1: A coarse mesh of a 2D wedge.

The upper boundary is modelled as an opening with an atmospheric pressure condition applied. The boundary on the left side of the domain is a symmetry plane allowing the simulation of half the wedge and therefore reducing the computational time taken to solve the problem. The wedge itself is modeled as a smooth wall, with a no slip condition. The simulation is carried out for varying mesh densities and turbulence models.

The simulation of a free falling wedge requires the inflow velocity to vary according to the vertical force (F) on the wedge. In order to calculate the new velocity (W_{NEW}), the velocity (W_{OLD}) at the previous time step (t) must be known. A FORTRAN program was integrated within the CFD simulation. At each time step the total vertical force acting on the wedge is known and using the wedge mass, a new velocity can be found as:

$$W_{NEW} = W_{OLD} + \left(g - \frac{F}{M} \right) \Delta t \ , \qquad (1)$$

where g is acceleration due to gravity, and M is the mass of the wedge.

As the necessary timestep for the CFD simulation is sufficiently small a simple first order calculation is suitably accurate.

3.2 Experimental Data

In order to analyse the predicted impact it is important to know the pressure distribution along the length of the wedge, as well as time histories of the impact pressures. Yettou et al (2006) conducted experiments on a free falling wedge. Parameters such as the drop height, deadrise angle and wedge mass are varied. Pressure is measured using 12 transducers distributed evenly along the wedge as illustrated in figure 2. The transducers are numbered from 1 near the wedge apex, to 12 near the edge of the wedge. Wedge position and velocity are also measured. These experimental data are used to validate the free falling wedge simulation described in section 4. Although different experiments with a variation in parameters such as drop height and wedge mass were conducted, one case in particular is analysed, as the pressure distribution on the wedge during impact is presented by Yettou et al (2006). A wedge with a mass of 94kg and a deadrise angle of 25° is dropped from a height of 1.3 metres. The impact velocity can be calculated to be 5 m/s.

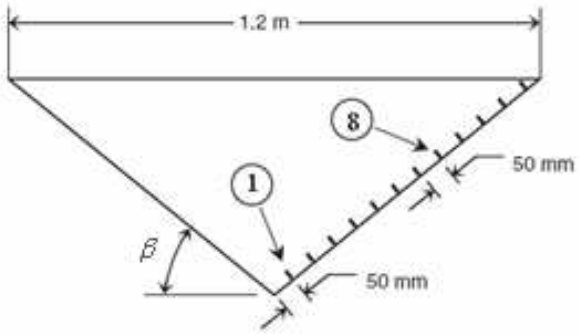

Figure 2: Experimental wedge used in drop tests, showing the pressure transducer positions and numbering system (adapted from Yettou et al, 2006).

4. Results

Initial inspection of the results is conducted in a qualitative manner. The free surface is inspected to ensure that a reasonably sharp interface is predicted with a rapid variation of volume fraction across 3 to 5 cells only. Figure 3 illustrates a typical free surface mid way through a simulation for the coarse mesh showing a contour plot of the water volume fraction. This was deemed acceptable with clear identification both of the wedge jet and mean water level.

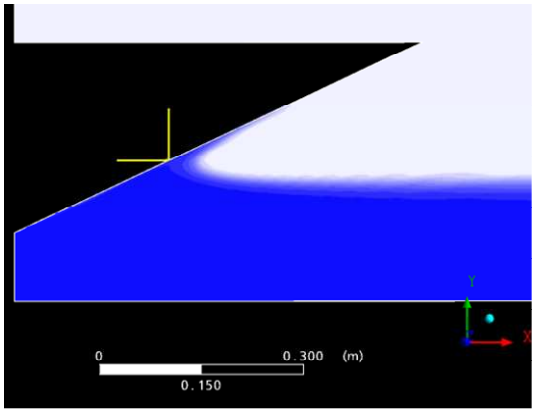

Figure 3: Contour plot of the water volume fraction illustrating the free surface.

The effects of turbulence model and other modelling parameters are investigated using a coarse mesh containing 9000 cells (illustrated in figure 1). There is only a slight difference between the k-ε, k-ε RNG and SST turbulence models. The best results are obtained using

the *k*- ε model with real air and with the solver set to double precision.

The effects of the number of mesh elements on the results are also studied. The experimental pressures measured by Yettou et al (2006) are assumed to be averaged over the diameter of the pressure transducer (19mm). Figure 4 presents a comparison of peak pressures, and averaged pressures at transducer 1. With a fine mesh containing 52000 cells, the averaged pressure gives a more accurate prediction of the experimental value than the peak pressure at the same point.

As the number of cells in the mesh is increased, the accuracy of the prediction of pressure along the wedge increases. It must be noted that this increase in accuracy is accompanied by an increase in computational cost.

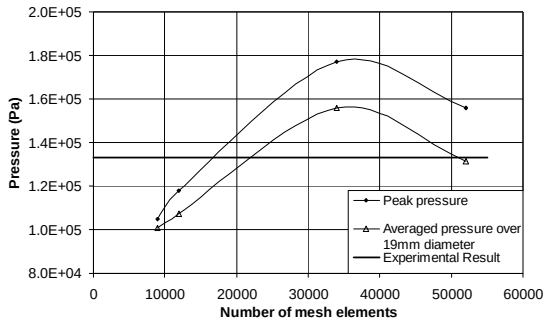

Figure 4: Comparison between peak and averaged pressures for different mesh densities.

Figure 5 presents the computed prediction of the pressure distribution along the wedge at 4 different times. These times correspond to the maximum pressure experienced by transducers 1, 3, 5 and 6. The time is set to zero when the wedge first touches the water. It is noted that each pressure transducer has a diameter of 19mm. Therefore the average maximum pressure over a 19mm section of the wedge must also be considered. The peak pressures are presented in figure 9 as well as the average maximum pressure at the position of each transducer.

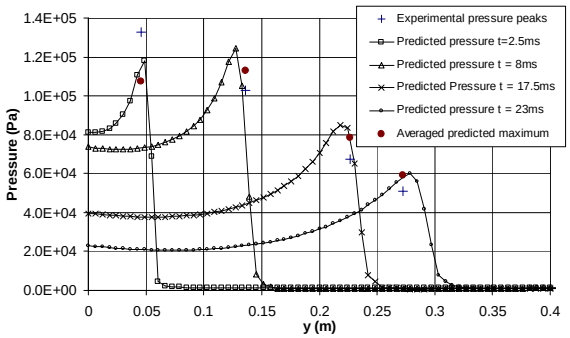

Figure 5: Predicted pressure distribution along the wedge face, with averaged maximum pressure and experimental data.

Peak pressures are under-predicted near the wedge apex, as is the averaged pressure. The pressures are over predicted as the water jet travels up the wedge and the averaged pressure follows the same trend, although with increased accuracy.

Although the pressure time history for each transducer is presented by Yettou et al (2006), the data is only given for the peak pressures. Figure 6 illustrates an adapted graph of the pressure time history presented by Yettou et al (2006). This can be compared with figure 7, the predicted pressure time histories at transducers 1, 3, 5 and 6. The graphs presented in figure 11 have the same vertical axis scale as those illustrated in figure 10. Over predicted peak values cannot be deduced from figure 7, but are presented in figure 5. The time that each impact occurs is well predicted.

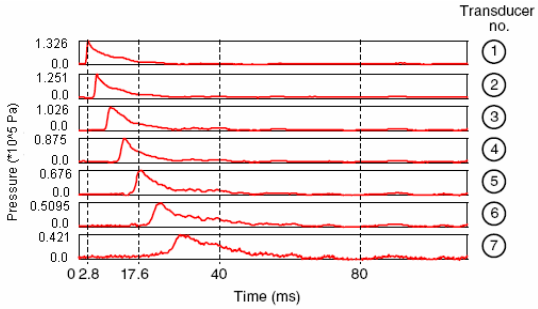

Figure 6: Graph of pressure time histories for transducers 1-7 (adapted from Yettou et al, 2006).

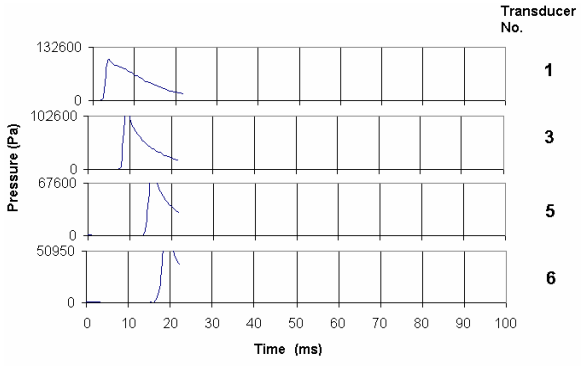

Figure 7: Predicted pressure time histories for transducers 1, 3, 5 and 6.

A possible reason for the inaccuracies near the wedge tip could be due to a large rate of change in the pressure experienced by the wedge. It is possible that modelling water as a compressible fluid could reduce this problem. A further possible source of error could be in the prediction of the surface tension of the water. A preliminary study is carried out to examine the effect of including a surface tension model. Figure 8 illustrates the contour plot of the free surface. It is noted that the water jet is much thinner along the wall of the wedge.

While the prediction of pressures acting on the wedge is important, the forces acting on the wedge and its subsequent motions are of primary concern in this study. Figure 9 illustrates the accuracy of various potential flow theories when compared to the experimental results and the current CFD predictions.

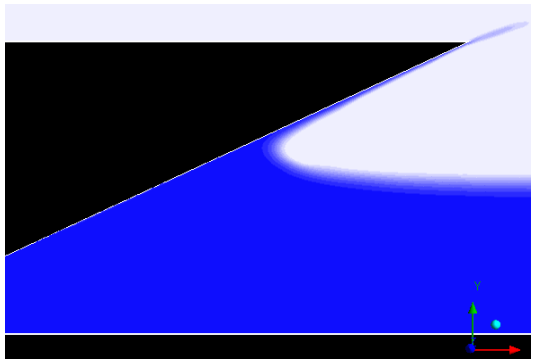

Figure 8: Contour plot of the water volume fraction illustrating the free surface with surface tension.

Both the experimental data and the CFD predictions differ from the potential theory in a similar manner. Initially, the wedge velocity is well predicted by the von Karman (1929) and Zarnick (1978) models. 25 ms after the impact, Zhao's (1996) model accurately predicts the wedge motion. The CFD predicts the wedge velocity well compared to experimental results from the

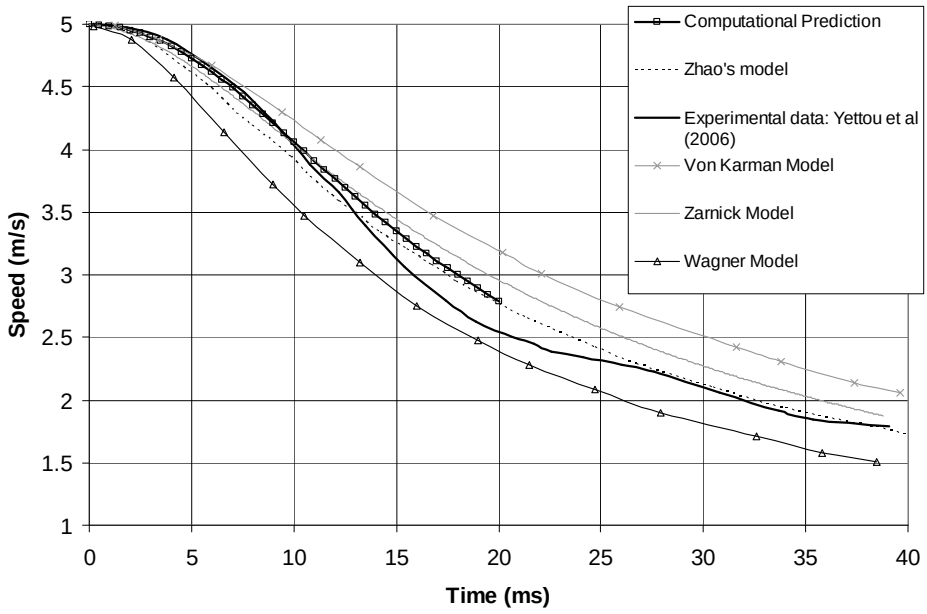

Figure 9: Comparison between computational prediction, experimental data and various potential flow solutions.

time of impact until 10ms after impact. After 10ms, the CFD predicts a similar velocity to Zhao's theoretical model.

5. Conclusions

A computational fluid dynamics method using the Reynold's averaged Navier-Stokes equations is applied to solve the problem of a two-dimensional wedge falling into water. The results presented demonstrate that such a CFD approach predicts the magnitude and time history of the pressure distribution accurately as compared to available experimental data. This in turn leads to an accurate prediction of the wedge speed as it enters the water. The latter is especially important when considering the overall motions of the wedge. The forces calculated using this model can then be applied in the equations of motion in the strip theory model as a replacement for those previously calculated using potential flow theories. The results presented illustrate an improvement over potential flow theory predictions. Future work involves the extension of the wedge impact model to calculate the forces on a number of wedges that can be linked together using strip theory to create a 3D model.

References

Akimoto, A., Miyata, H., (2002). 'Finite-volume simulation to predict the performance of a sailing boat'. Journal of Marine Science and Technology **7** pp 31-42.

Ansys CFX (2007). CFX version 11. Further information available at http://www.ansys.com/products/cfx.asp.

Azcueta, R. (2002) 'RANSE simulations for sailing yachts including dynamic sinkage & trim and unsteady motions in waves'. High Performance Yacht Design Conference, Auckland.

Azcueta, R. (2003). 'Steady and unsteady RANSE simulations for planing craft' in the 7th Conference on Fast Sea Transportation, FAST'03, Ischia, Italy.

Lewis, S.G., Hudson, D. A., Turnock, S. R., Blake, J. I. R. & Shenoi, R. A. (2006) 'Predicting Motions of High Speed RIBs: A Comparison of Non-linear Strip Theory with Experiments' Proceedings of the 5th International Conference on High Performance Marine Vehicles (HIPER '06) pp 210-224.

Launder, B., Spalding, D. (1974). 'The Numerical Computation of Turbulent Flows'. Computer Methods in Applied Mechanics and Engineering, 3 pp269-289.

Menter, F.R. (1994) 'Two-Equation Eddy-Viscosity Turbulence models for Engineering Applications'. AIAA Journal 32(8) pp 1598-1605, August.

Ohmori, T., (1998). 'Finite-volume simulation of flows about a ship in maneuvering motion' Journal of Marine Science and Technology 3 pp 82-93.

Sato, Y., Miyata, H., & Sato, T. (1999). 'CFD simulation of 3-dimensional motion of a ship in waves: application to an advancing ship in regular waves'. Journal of Marine Science and Technology 4 pp 108-116.

Von Karman, T. (1929): 'The impact of seaplane floats during landing'. Technical Report TN-321. NACA.

Wagner, H. (1932). 'Über Stross-und Gleitvorgänge an der Oberfläche von Flüssigkeiten', ZAMM, **12**, 4, pp. 193–215.

WS Atkins Consultants. (2003). 'MARNET best practice guidelines for marine applications of computational fluid dynamics'. Technical report, MARNET.

Yettou, E-M., Desrochers, A., Champoux, Y. (2006). 'Experimental study on the water impact of a symmetrical wedge'. Fluid Dynamics Research 38 pp47-66.

Zarnick, E.E. (1978). 'A Non-Linear Mathematical Model of Motions of a Planing Boat in Regular waves'. Technical report. DTNSRDC-78/032. David Taylor Naval Ship Research and Development Center.

Zhao, R., Faltinsen, O., & Aarsnes, J., (1996). 'Water entry of arbitrary two-dimensional sections with and without separation'. In Proceedings of 21st Symposium on Naval Hydrodynamics pp 408-423, Washington D.C.